Supplementary Material for "SICKLE: A Multi-Sensor Satellite Imagery Dataset Annotated with Multiple Key Cropping Parameters"

Depanshu Sani[1], Sandeep Mahato[2], Sourabh Saini[1], Harsh Kumar Agarwal[1],
Charu Chandra Devshali[2], Saket Anand[1], Gaurav Arora[1], Thiagarajan Jayaraman[2]
[1]Indraprastha Institute of Information Technology, Delhi, India
[2]MS Swaminathan Research Foundation, Chennai, India
https://sites.google.com/iiitd.ac.in/sickle/home

1. Rationale for Location and Crop Selection

We study paddy cultivation in the Cauvery Delta, which is considered to be a major paddy cultivation region in Tamil Nadu, India, which supports food security and livelihoods among millions of farmers in the region [1]. In any given agricultural year, the farmers in our study region are primarily dependent on irrigation from surface-water and groundwater sources. Additionally, they rely on two monsoon seasons for rainfall: the Southwest Monsoon, which occurs from June to September, and the Northeast Monsoon, from October to December. Regarding the agricultural practices in the Delta, they are intrinsically aligned with a "water availability" calendar. To illustrate this, in a typical agricultural year, farmers base their decisions on whether to cultivate one or two paddy crops on the availability of water. These decisions are influenced by a variety of factors, including surface and groundwater irrigation, as well as the predictable timing of the Southwest Monsoon (June-September) and Northeast Monsoon (October-December). Therefore, the Delta's agricultural system has been shaped over time to adapt to this water availability calendar.

There's growing evidence that points towards significant shifts in the Delta's agrarian landscape, specifically the stagnation in paddy yields and an uncertainty in water availability for paddy cultivation [3]. An Indian Council for Agricultural Research (ICAR) study in 2013 reclassified the four districts of the Cauvery delta from dry semi-humid to semi-arid conditions [2]. In the context of these changes reported for the region and its centrality to rice production, understanding these emerging variations and challenges in paddy cultivation in the Delta becomes crucial.

2. Spatial Distribution and Sampling Methods

The Cauvery Delta Zone (CDZ) as shown in Fig 1 spans across four principal districts: Thiruvarur, Thanjavur, Nagapattinam, and Mayiladuthurai of Tamil Nadu, India. Collectively, these districts make up 57% of the CDZ. The alluvial soils within this region are prime for wet rice cultivation, complemented by the ancient irrigation system of the Cauvery delta [3]. Integral irrigation structures like the Grand Anicut and the Mettur dam ensure the distribution of water to these districts.

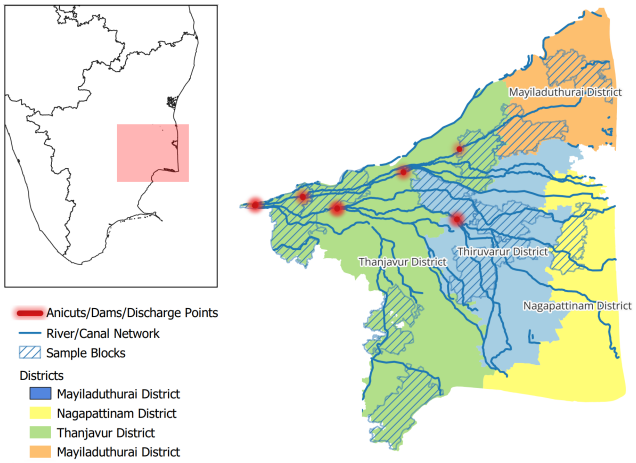

Figure 1. The study region is part of the Cauvery Delta Zone (CDZ). The sample taluks highlighted in the map are taluks from where field samples were collected for the study.

2.1. Data Collection Blocks

The blocks for data collection, outlined in Table 1, are sub-district administrative divisions positioned across the downstream parts of the Vennar and Cauvery rivers. Their selection was guided by the criticality of irrigation water availability, influenced by river flows managed by a series of dams and anicuts (Fig 1). The timing of water release and its downstream availability profoundly impacts paddy crop sowing dates across the Delta [4].

Block	District	Region (by source of irrigation)	Phase
Thiruvaiyaru	Thanjavur	Upper Cauvery	Phase One
Kordacheri	Thanjavur	Middle Vennar	Phase Two
Sethubavasathiram	Thanjavur	Coastal GAC	Phase Two
Thiruvidaimaruthur	Thanjavur	Middle Cauvery	Phase Two
Thiruvonam	Thanjavur	Coast GAC	Both Phase
Valangaiman	Thiruvarur	Middle Vennar	Phase One
Mannargudi	Thiruvarur	Middle Vennar	Phase One
Kilvelur	Nagapattinam	Coastal Vennar	Both Phase
Kuthalam	Mayiladuthurai	Middle Cauvery	Phase One
Sirkali	Mayiladuthurai	Coastal Cauvery	Phase Two

Table 1. List of blocks and the districts where data collection was conducted in the Delta. GAC refers to the Grand Anicut Canal. Upper, Middle and Coastal refer to a rough three-fold division of the length of the Cauvery and Vennar downstream of the Grand Anicut, from where also the GAC originates.

2.2. Field Data Collection

1. **Phase One (2018-2020):** Emphasis on collecting crop-type information at the plot level. This data helps classify paddy and non-paddy plots, detailing various crop types and their sowing and harvesting periods under different seasons.
2. **Phase Two (2019-2020):** Emphasis on detailed information on paddy cultivation, specifically yield data, which is instrumental for the calibration and validation of the proposed remote-sensing-based paddy yield prediction model. The collection was limited to two years to reduce the possibility of errors in the yield records.

All data was consolidated from farmer interviews, structured questionnaires, and the Kobo Collect android app.

3. Directory Structure

The dataset is organized according to the following directory structure. Considering we want to fetch Landsat-8's image of band B1 acquired on $2018 - 06 - 16$ for the 1^{st} sample, the path will be `L8/1/LC08_142052_20180616/LC08_142052_20180616.SR_B1.tif`, shown in the parenthesis.

Satellite Name (*L8*)
- **Sample ID** (*1*)
  - **Date** (*LC08_142052_20180616*)
    - **BandID.tif** (*LC08_142052_20180616.SR_B1.tif*)
    - ⋮
  - ⋮
- ⋮
- **Metadata** (*metadata.pkl*)

4. Dataset Analysis

Fig 2 presents the pixel-wise key crop parameters' distribution for the dataset using the split strategy based on the Wasserstein distance. Fig 5 presents the statistics of the entire dataset. It includes the various types of crops that are cultivated in the Cauvery Delta region in Tamil Nadu, the area of each plot in acre, regional standard seasons (Table 2) present in the dataset that are mapped using [5], and the total number of samples in each district. Fig 4 shows a more fine-grained dataset analysis at a block level. Along with other statistics, Fig 4 also contains the distribution of crop yield for each block. Figure 3 demonstrates a sample input from the dataset. A few images acquired on the dates mentioned on the axis are visualized in the figure, along with the collected phenology dates. As in this example sample, there are cases where multiple images from different satellites are available on the same day, but no images on the sowing, transplanting and harvesting are available.

5. Additional Experiments and Results

Tables 3 - 24 include benchmarking results for various state-of-the-art methods on single and time-series image prediction tasks. For single-image tasks, we present the results using U-Net 2D and DeepLabV3+, and for time-series tasks, we present the results using U-Net 3D, ConvLSTM and U-TAE. Fusion was not performed for single-image tasks because it is unlikely to capture images from multiple satellites on the same day (or within a small time window) because of their low revisit frequency. Crop signatures change significantly within a few days, and hence, it is not ideal to fuse the image of one satellite with the nearest available image from another satellite. The best results are highlighted in **green** and the competing (second best) are represented using a **bold font**.

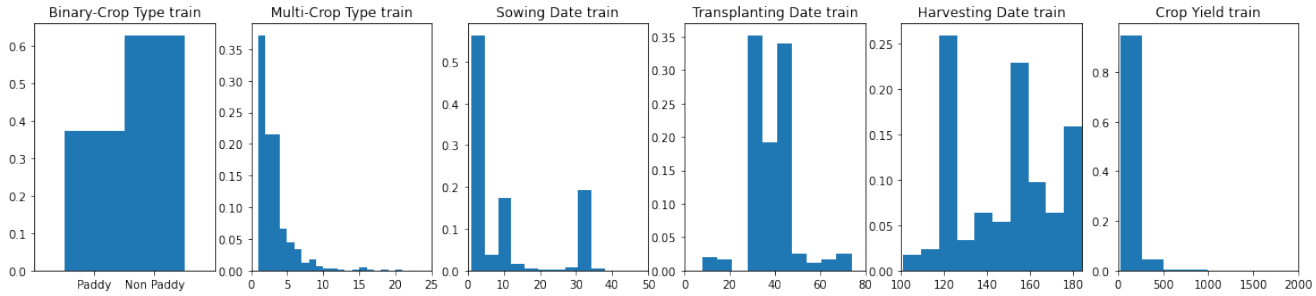

(a) Training Set

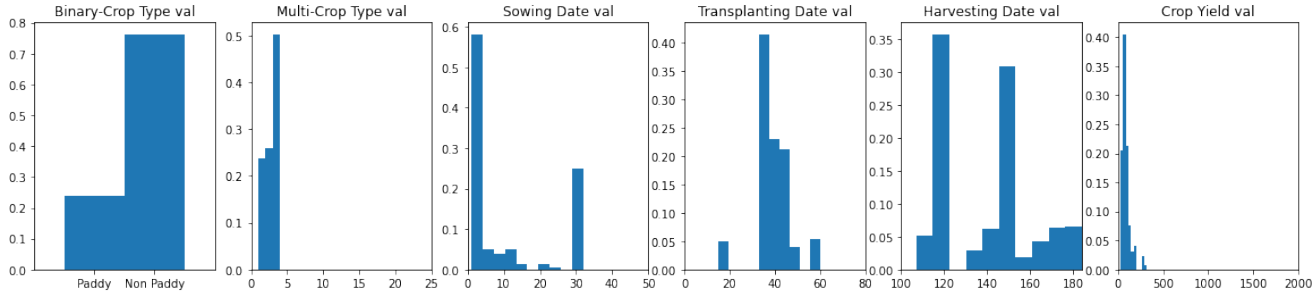

(b) Validation Set

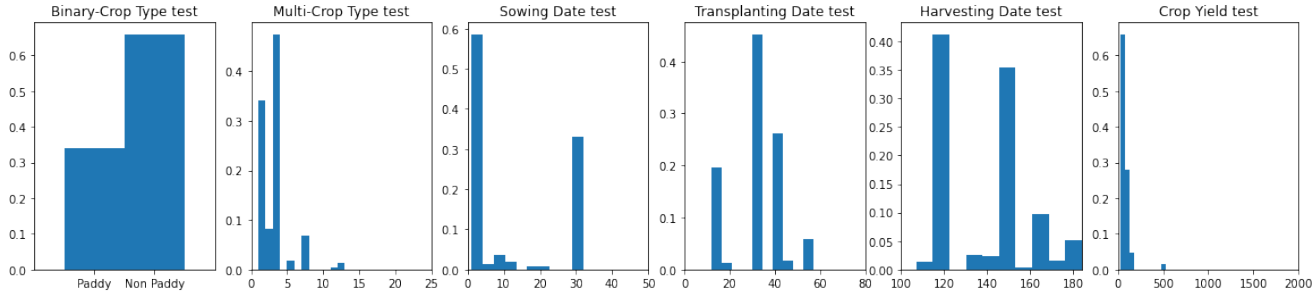

(c) Testing Set

Figure 2. **Data distribution of training, validation and test sets.** Distribution of the pixel-wise annotations for all the key crop parameters using the split based on Wasserstein distance. Here, the Y-axis denotes the percentage of total number of pixels and the X-axis denotes the crop type, phenology dates and crop yield. It can be observed that the distribution of various crop parameters is approximately the same across all the sets using this technique.

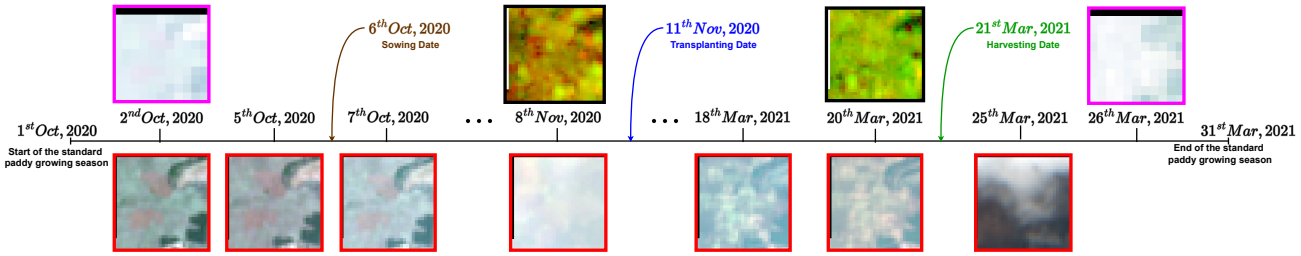

Figure 3. **Sample input from the dataset.** The axis denotes the individual days from the start of the paddy growing season till the end of that season. The extreme ends of this axis represent the start and the end of the regional standard season. We visualize a few image patches acquired on the corresponding dates from different satellites. Images with pink boundaries denote images acquired from Landsat-8, black boundaries denote Sentinel-1 and red boundaries denote Sentinel-2. Multiple observations from different satellites are observed on various dates. It is also possible to get multiple observations from different satellites on the same day, as shown in the figure. Moreover, as in this case, there may be no images on the sowing, transplanting and/or harvesting dates.

Season	Sowing Month	Duration (days)
Navarai	Dec. - Jan.	120
Sornavari	Apr. - May.	120
Early Kar	Apr. - May.	120
Kar	May. - June	120
Kuruvai	June - July	120
Early Samba	July - Aug.	135
Samba	Aug.	180
Late Samba	Sep. - Oct.	135
Thaladi	Sep. - Oct.	135
Late Pishanam	Sep. - Oct.	135
Late Thaladi	Oct. - Nov.	120

Table 2. Regional standard growing seasons for paddy cultivation in the Cauvery Delta region obtained from Tamil Nadu Agricultural University (TNAU) [5]. The time-series dataset is created using the maximum duration of the growing paddy season.

References

[1] Tamilarasu Arivelarasan, V. S. Manivasagam, Vellingiri Geethalakshmi, Kulanthaivel Bhuvaneswari, Kiruthika Natarajan, Mohan Balasubramanian, Ramasamy Gowtham, and Raveendran Muthurajan. How far will climate change affect future food security? an inquiry into the irrigated rice system of peninsular india. *Agriculture*, 13(3), 2023. 1

[2] B. M. K. Raju, K. V. Rao, B. Venkateswarlu, A. V. M. S. Rao, C. A. Rama Rao, V. U. M. Rao, B. Bapuji Rao, N. Ravi Kumar, R. Dhakar, N. Swapna, and P. Latha. Revisiting climatic classification in india: a district-level analysis. *Current Science*, 105(4):492–495, 2013. 1

[3] V. Surjit. Cropping Pattern and Farming Practices in Palakurichi Village, 1918–2004. *Journal*, 1(1):43–62, January-J 2011. 1

[4] V. Surjit. A century of agrarian change in lower cauvery delta: A study of palakurichi village 1918-2018. *National Institute of Rural Development and Panchayati Raj, Ministry of Rural Development, Govt. of India*, 2023. 1

[5] Season and varieties :: Rice, 2013. Tamil Nadu Agricultural University. 2, 4

Satellite	L8	S2	S1
OA Accuracy	69.69% ± 2.56%	**75.19% ± 3.27%**	**80.16% ± 2.71%**
Paddy Accuracy	54.85% ± 11.49%	62.45% ± 2.95%	72.18% ± 13.95%
Non-Paddy Accuracy	74.53% ± 6.57%	80.29% ± 5.60%	84.23% ± 4.10%
OA F1 Score	62.70% ± 1.89%	**70.64% ± 2.60%**	**77.78% ± 3.86%**
Paddy F1 Score	46.74% ± 4.58%	59.13% ± 2.29%	70.62% ± 6.45%
Non-Paddy F1 Score	78.65% ± 2.81%	82.14% ± 2.95%	84.93% ± 1.51%
OA IoU	47.73% ± 1.77%	**55.89% ± 3.23%**	**64.35% ± 4.82%**
Paddy IoU	30.59% ± 3.83%	42.01% ± 2.29%	54.87% ± 7.74%
Non-Paddy IoU	64.88% ± 3.80%	69.77% ± 4.24%	73.83% ± 2.26%

Table 3. **Single-Image Crop Segmentation task using U-Net 2D architecture.** All the images within the *regional standard growing season* are used as separate input for the crop type segmentation task.

Satellite	L8	S2	S1
OA Accuracy	71.17% ± 1.64%	**74.67% ± 2.37%**	**82.35% ± 1.64%**
Paddy Accuracy	51.03% ± 11.93%	57.70% ± 10.15%	77.26% ± 8.44%
Non-Paddy Accuracy	77.76% ± 5.29%	81.47% ± 5.37%	84.94% ± 1.92%
OA F1 Score	63.15% ± 2.58%	**69.21% ± 2.58%**	**80.51% ± 2.39%**
Paddy F1 Score	46.09% ± 5.96%	56.35% ± 4.48%	74.55% ± 3.96%
Non-Paddy F1 Score	80.21% ± 1.89%	82.07% ± 2.11%	86.46% ± 0.84%
OA IoU	48.53% ± 2.02%	**54.48% ± 2.77%**	**67.85% ± 3.11%**
Paddy IoU	30.08% ± 4.85%	39.32% ± 4.38%	59.55% ± 4.95%
Non-Paddy IoU	66.98% ± 2.62%	69.64% ± 3.03%	76.15% ± 1.31%

Table 4. **Single-Image Crop Segmentation task using DeepLabV3+ architecture.** All the images within the *regional standard growing season* are used as separate input for the crop type segmentation task.

Satellite	L8	S2	S1	Fusion
OA Accuracy	75.27% ± 4.12%	89.06% ± 1.80%	**91.05% ± 3.71%**	**90.65% ± 3.18%**
Paddy Accuracy	54.99% ± 14.66%	80.80% ± 6.29%	82.46% ± 8.41%	82.93% ± 7.14%
Non-Paddy Accuracy	85.50% ± 8.58%	93.23% ± 1.32%	95.38% ± 4.20%	94.54% ± 3.39%
OA F1 Score	70.57% ± 5.40%	87.50% ± 2.32%	**89.71% ± 4.20%**	**89.32% ± 3.61%**
Paddy F1 Score	59.11% ± 9.22%	83.10% ± 3.46%	86.02% ± 5.68%	85.56% ± 4.88%
Non-Paddy F1 Score	82.02% ± 3.56%	91.90% ± 1.19%	93.40% ± 2.78%	93.07% ± 2.37%
OA IoU	56.04% ± 5.84%	78.12% ± 3.48%	**81.77% ± 6.60%**	**81.07% ± 5.77%**
Paddy IoU	42.43% ± 8.99%	71.20% ± 4.96%	75.81% ± 8.51%	75.02% ± 7.49%
Non-Paddy IoU	69.65% ± 5.09%	85.04% ± 2.04%	87.73% ± 4.77%	87.12% ± 4.13%

Table 5. **Time-Series Crop Segmentation task using U-Net 3D architecture.** The time-series data prepared using the proposed method is used as an input for the crop type segmentation task.

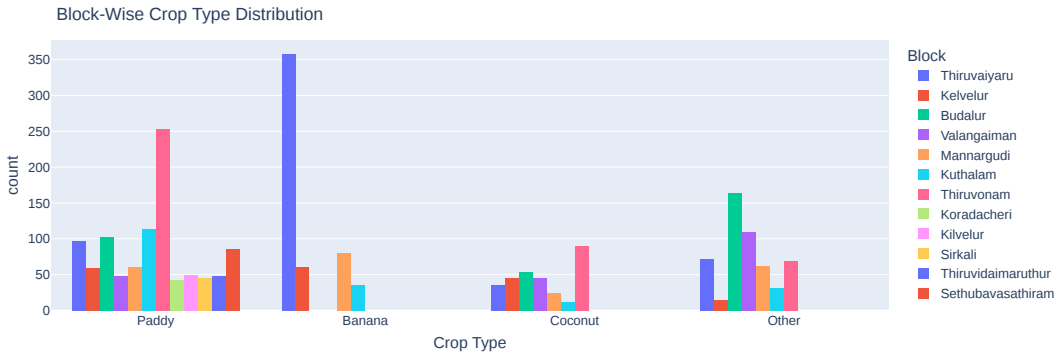

(a)

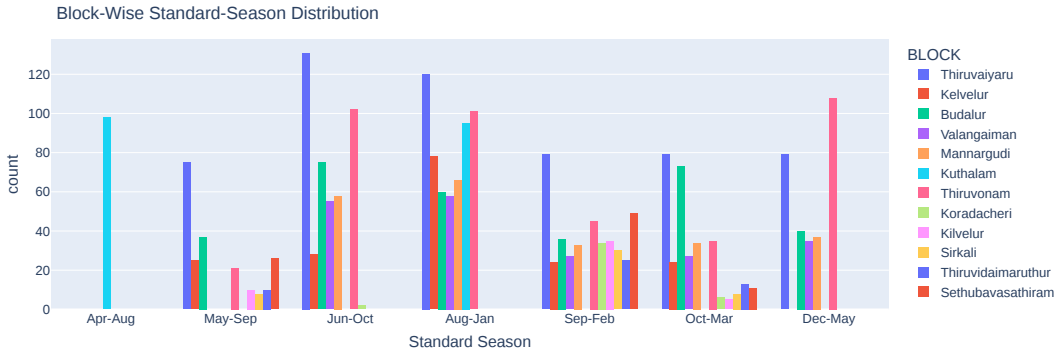

(b)

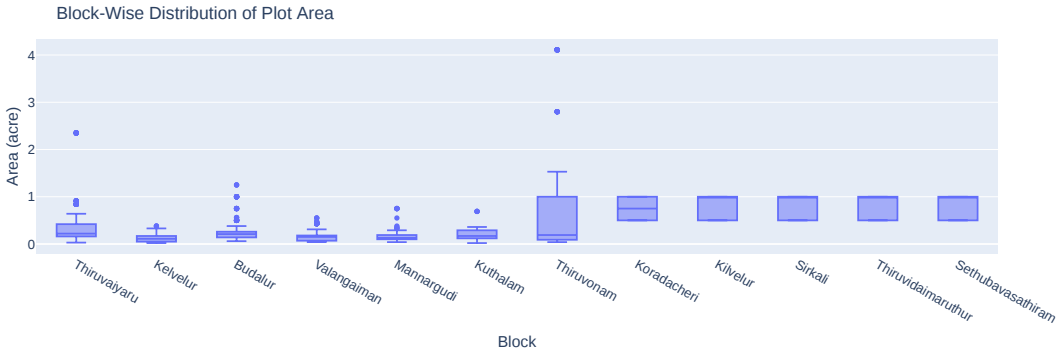

(c)

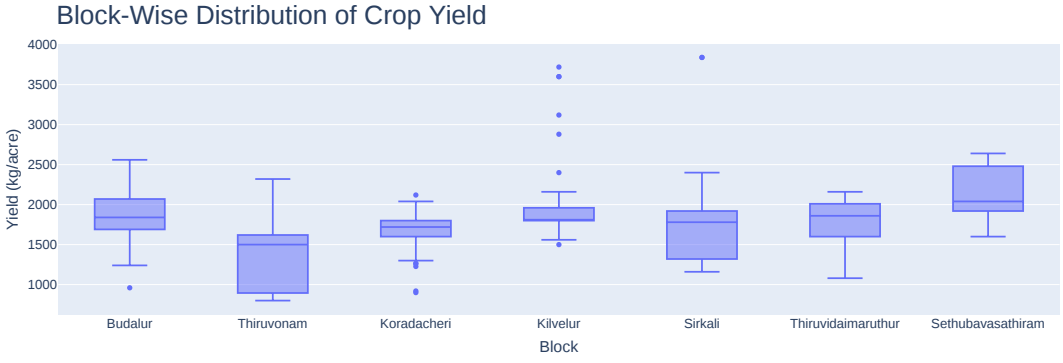

(d)

Figure 4. Block-Level Dataset Statistics. Figure 4a shows the distribution of various types of crops in the dataset that are cultivated in the study region in each of the studied blocks. Figure 4c represents the area (in acre) of each of the 388 individual plots in the block. Figure 4b shows the distribution of the standard paddy seasons observed in the study region for each block. Figure 4d shows the block-wise distribution of the crop yield.

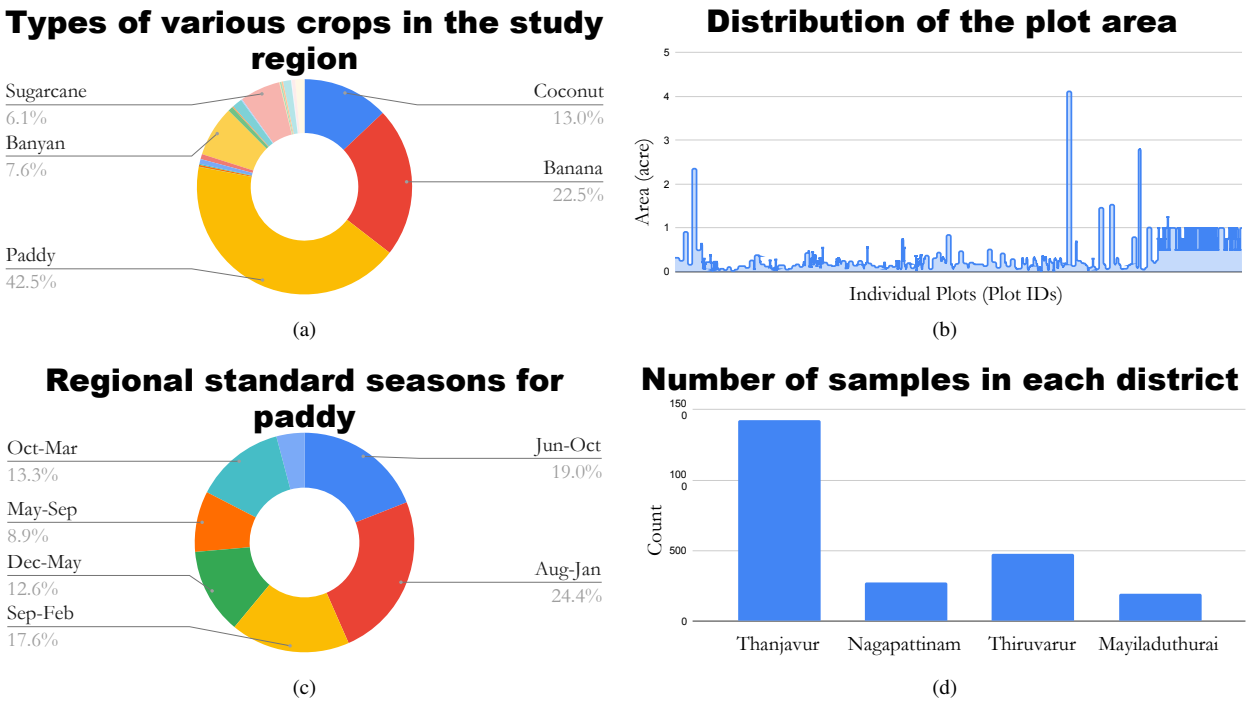

Figure 5. Dataset Statistics. Figure 5a shows the distribution of various types of crops in the dataset that are cultivated in the study region. Figure 5b represents the area (in acre) of each of the 388 individual plots. X-axis denotes the plot id of each plot and Y-axis denotes the area (in acre). Figure 5c shows distribution of the standard paddy seasons observed in the study region. Figure 5d shows the district-wise distribution of the collected $2,370$ samples.

Satellite	L8	S2	S1	Fusion
OA Accuracy	**77.03% ± 4.00%**	70.87% ± 5.44%	75.33% ± 9.70%	**76.28% ± 5.31%**
Paddy Accuracy	63.55% ± 28.73%	32.23% ± 15.44%	41.25% ± 31.55%	54.17% ± 5.24%
Non-Paddy Accuracy	83.83% ± 12.15%	90.34% ± 6.84%	92.52% ± 5.31%	87.42% ± 8.99%
OA F1 Score	**72.39% ± 7.90%**	60.85% ± 8.43%	65.27% ± 18.52%	**71.81% ± 4.64%**
Paddy F1 Score	61.98% ± 15.34%	41.24% ± 14.47%	46.96% ± 32.20%	60.75% ± 4.87%
Non-Paddy F1 Score	82.80% ± 3.28%	80.46% ± 3.74%	83.57% ± 5.56%	82.88% ± 4.72%
OA IoU	**58.52% ± 8.38%**	47.15% ± 8.10%	53.64% ± 17.21%	**57.37% ± 5.58%**
Paddy IoU	46.30% ± 15.70%	26.88% ± 12.41%	35.18% ± 26.91%	43.76% ± 4.93%
Non-Paddy IoU	70.75% ± 4.65%	67.43% ± 5.30%	72.09% ± 8.11%	70.97% ± 6.65%

Table 6. **Time-Series Crop Segmentation task using ConvLSTM architecture.** The time-series data prepared using the proposed method is used as an input for the crop type segmentation task.

Satellite	L8	S2	S1	Fusion
OA Accuracy	73.80% ± 4.32%	66.36% ± 0.20%	**82.12% ± 2.39%**	**77.51% ± 5.66%**
Paddy Accuracy	27.99% ± 16.28%	0.04% ± 0.09%	68.88% ± 7.96%	54.68% ± 19.18%
Non-Paddy Accuracy	96.90% ± 3.16%	99.80% ± 0.31%	88.80% ± 2.09%	89.02% ± 12.47%
OA F1 Score	61.13% ± 12.06%	39.93% ± 0.12%	**79.39% ± 3.09%**	**72.23% ± 7.03%**
Paddy F1 Score	39.09% ± 22.23%	0.08% ± 0.18%	71.92% ± 4.69%	60.70% ± 11.72%
Non-Paddy F1 Score	83.16% ± 2.10%	79.78% ± 0.15%	86.87% ± 1.61%	83.77% ± 5.39%
OA IoU	48.58% ± 8.83%	33.20% ± 0.11%	**66.57% ± 4.17%**	**58.37% ± 8.06%**
Paddy IoU	25.94% ± 14.92%	0.04% ± 0.09%	56.33% ± 5.96%	44.38% ± 12.06%
Non-Paddy IoU	71.21% ± 3.05%	66.36% ± 0.20%	76.81% ± 2.56%	72.35% ± 7.60%

Table 7. **Time-Series Crop Segmentation task using U-TAE architecture.** The time-series data prepared using the proposed method is used as an input for the crop type segmentation task.

Satellite	RMSE	MAE	MAPE
L8	3.63 ± 0.64	2.66 ± 0.96	1.45% ± 0.53%
S2	3.22 ± 0.59	**2.30 ± 0.61**	1.26% ± 0.33%
S1	4.50 ± 1.14	3.61 ± 0.90	1.97% ± 0.49%
Fusion	3.61 ± 0.59	**2.33 ± 0.64**	1.27% ± 0.35%

Table 8. **Sowing Date prediction task using U-Net 3D architecture.** The time-series data prepared using the proposed method is used as an input for predicting the sowing date of the paddy crops.

Satellite	RMSE	MAE	MAPE
L8	6.23 ± 1.839	5.13 ± 1.821	2.81% ± 1.00%
S2	3.38 ± 0.075	**2.90 ± 0.111**	1.59% ± 0.06%
S1	4.94 ± 0.231	3.77 ± 0.519	2.06% ± 0.28%
Fusion	3.61 ± 0.687	**2.91 ± 0.454**	1.59% ± 0.25%

Table 9. **Sowing Date prediction task using ConvLSTM architecture.** The time-series data prepared using the proposed method is used as an input for predicting the sowing date of the paddy crops.

Satellite	RMSE	MAE	MAPE
L8	5.72 ± 0.36	3.88 ± 0.33	2.12% ± 0.18%
S2	3.55 ± 0.36	**2.97 ± 0.34**	1.62% ± 0.19%
S1	4.95 ± 0.10	3.22 ± 0.15	1.76% ± 0.08%
Fusion	3.86 ± 0.71	**2.91 ± 0.62**	1.59% ± 0.34%

Table 10. **Sowing Date prediction task using U-TAE architecture.** The time-series data prepared using the proposed method is used as an input for predicting the sowing date of the paddy crops.

Satellite	RMSE	MAE	MAPE
L8	9.50 ± 2.635	**6.20 ± 1.030**	3.39% ± 0.56%
S2	9.45 ± 2.475	6.36 ± 2.164	3.48% ± 1.18%
S1	10.67 ± 1.039	7.23 ± 0.779	3.95% ± 0.43%
Fusion	9.28 ± 2.312	**6.16 ± 1.770**	3.37% ± 0.97%

Table 11. **Transplanting Date prediction task using U-Net 3D architecture.** The time-series data prepared using the proposed method is used as an input for predicting the transplanting date of the paddy crops.

Satellite	RMSE	MAE	MAPE
L8	14.50 ± 0.93	9.41 ± 0.48	$5.14\% \pm 0.26\%$
S2	11.17 ± 0.31	$\mathbf{7.47 \pm 0.27}$	$4.08\% \pm 0.15\%$
S1	12.11 ± 0.90	8.37 ± 0.53	$4.57\% \pm 0.29\%$
Fusion	11.62 ± 0.93	$\mathbf{7.34 \pm 0.59}$	$4.01\% \pm 0.32\%$

Table 12. **Transplanting Date prediction task using ConvLSTM architecture.** The time-series data prepared using the proposed method is used as an input for predicting the transplanting date of the paddy crops.

Satellite	RMSE	MAE	MAPE
L8	11.56 ± 1.25	8.75 ± 0.97	$4.78\% \pm 0.53\%$
S2	10.66 ± 0.78	$\mathbf{7.33 \pm 0.76}$	$4.01\% \pm 0.41\%$
S1	11.38 ± 0.14	7.60 ± 0.18	$4.15\% \pm 0.10\%$
Fusion	9.83 ± 1.69	$\mathbf{6.62 \pm 1.23}$	$3.62\% \pm 0.67\%$

Table 13. **Transplanting Date prediction task using U-TAE architecture.** The time-series data prepared using the proposed method is used as an input for predicting the transplanting date of the paddy crops.

Satellite	RMSE	MAE	MAPE
L8	12.99 ± 1.77	$\mathbf{9.86 \pm 0.74}$	$5.39\% \pm 0.40\%$
S2	11.51 ± 1.69	$\mathbf{8.83 \pm 1.52}$	$4.82\% \pm 0.83\%$
S1	13.17 ± 0.67	10.08 ± 0.56	$5.51\% \pm 0.31\%$
Fusion	14.09 ± 3.88	10.75 ± 3.39	$5.87\% \pm 1.85\%$

Table 14. **Harvesting Date prediction task using U-Net 3D architecture.** The time-series data prepared using the proposed method is used as an input for predicting the harvesting date of the paddy crops.

Satellite	RMSE	MAE	MAPE
L8	23.97 ± 2.71	20.14 ± 2.29	$11.00\% \pm 1.25\%$
S2	19.30 ± 4.26	$\mathbf{16.40 \pm 3.32}$	$8.96\% \pm 1.82\%$
S1	19.92 ± 2.71	17.52 ± 2.10	$9.57\% \pm 1.14\%$
Fusion	17.92 ± 1.82	$\mathbf{15.00 \pm 1.72}$	$8.20\% \pm 0.94\%$

Table 15. **Harvesting Date prediction task using ConvLSTM architecture.** The time-series data prepared using the proposed method is used as an input for predicting the harvesting date of the paddy crops.

Satellite	RMSE	MAE	MAPE
L8	18.61 ± 2.49	15.28 ± 2.11	$8.35\% \pm 1.15\%$
S2	13.47 ± 1.52	11.10 ± 1.13	$6.06\% \pm 0.62\%$
S1	13.01 ± 0.40	$\mathbf{9.97 \pm 0.54}$	$5.45\% \pm 0.30\%$
Fusion	13.10 ± 1.13	$\mathbf{10.48 \pm 1.24}$	$5.73\% \pm 0.67\%$

Table 16. **Harvesting Date prediction task using U-TAE architecture.** The time-series data prepared using the proposed method is used as an input for predicting the harvesting date of the paddy crops.

Satellite	RMSE	MAE	MAPE
L8	1165.91 ± 112.10	860.61 ± 71.31	$\mathbf{46.74}\% \pm \mathbf{3.82}\%$
S2	1462.35 ± 242.51	1080.82 ± 245.65	$60.44\% \pm 14.50\%$
S1	1206.86 ± 121.01	877.50 ± 121.64	$\mathbf{48.35}\% \pm \mathbf{7.64}\%$

Table 17. **Single image crop yield prediction task using U-Net 2D architecture.** Image that is available just before the harvesting date is used for estimating the yield of the paddy crops.

Satellite	RMSE	MAE	MAPE
L8	1222.90 ± 59.27	877.65 ± 36.90	**46.90**% $\pm$ **1.80**%
S2	1526.32 ± 240.54	1099.90 ± 160.51	$63.19\% \pm 11.01\%$
S1	1412.41 ± 137.34	1016.65 ± 81.09	**55.37**% $\pm$ **4.08**%

Table 18. **Single image crop yield prediction task using DeepLabV3+ architecture.** Image that is available just before the harvesting date is used as separate input for estimating the yield of the paddy crops.

Satellite	RMSE	MAE	MAPE
L8	1353.83 ± 151.97	968.43 ± 129.89	**54.00**% $\pm$ **9.67**%
S2	1574.40 ± 113.52	1209.35 ± 87.00	$72.38\% \pm 8.74\%$
S1	1533.31 ± 217.31	1144.96 ± 195.39	$71.81\% \pm 17.27\%$
Fusion	1484.82 ± 239.34	1131.55 ± 194.96	**70.35**% $\pm$ **13.75**%

Table 19. **Crop yield prediction with regional standard season using U-Net 3D architecture.** The time-series data prepared using the proposed method is used as an input for estimating the yield of the paddy crops when using the *regional standard growing season*.

Satellite	RMSE	MAE	MAPE
L8	$88.37 \pm 4.70\%$	$70.79 \pm 6.80\%$	$64.10\% \pm 4.70\%$
S2	$74.34 \pm 4.70\%$	$52.27 \pm 6.80\%$	**62.75**% $\pm$ **6.80**%$\pm$
S1	$41.70 \pm 4.70\%$	$33.02 \pm 6.80\%$	**59.98**% $\pm$ **5.34**%
Fusion	$72.27 \pm 4.70\%$	$31.01 \pm 6.80\%$	$63.89\% \pm 3.20\%$

Table 20. **Crop yield prediction with regional standard season using ConvLSTM architecture.** The time-series data prepared using the proposed method is used as an input for estimating the yield of the paddy crops when using the *regional standard growing season*.

Satellite	RMSE	MAE	MAPE
L8	1294.97 ± 85.22	908.09 ± 54.81	**50.40**% $\pm$ **4.41**%
S2	1342.07 ± 66.27	985.42 ± 69.44	$56.51\% \pm 6.71\%$
S1	1331.32 ± 90.26	914.01 ± 61.61	$52.78\% \pm 8.12\%$
Fusion	1242.00 ± 119.18	884.60 ± 103.12	**49.63**% $\pm$ **7.95**%

Table 21. **Crop yield prediction with regional standard season using U-TAE architecture.** The time-series data prepared using the proposed method is used as an input for estimating the yield of the paddy crops when using the *regional standard growing season*.

Satellite	RMSE	MAE	MAPE
L8	1402.42 ± 306.53	1024.57 ± 215.73	**59.38**% $\pm$ **14.75**%
S2	1590.68 ± 155.93	1211.72 ± 139.84	$73.59\% \pm 9.81\%$
S1	1493.99 ± 257.70	1096.79 ± 223.64	$65.66\% \pm 16.24\%$
Fusion	1426.34 ± 187.12	1085.44 ± 202.35	**64.56**% $\pm$ **13.77**%

Table 22. **Crop yield prediction with actual growing season using U-Net 3D architecture.** The time-series data prepared using the proposed method is used as an input for estimating the yield of the paddy crops when using the *actual standard growing season*.

Satellite	RMSE	MAE	MAPE
L8	1353.81 ± 142.08	990.63 ± 113.83	$59.92\% \pm 10.60\%$
S2	1411.31 ± 105.86	1019.06 ± 76.15	$60.83\% \pm 6.71\%$
S1	1260.50 ± 62.30	896.78 ± 62.11	**52.46**% $\pm$ **6.36**%
Fusion	1540.05 ± 276.92	1146.27 ± 203.53	$72.35\% \pm 12.67\%$

Table 23. **Crop yield prediction with actual growing season using ConvLSTM architecture.** The time-series data prepared using the proposed method is used as an input for estimating the yield of the paddy crops when using the *actual standard growing season*.

Satellite	RMSE	MAE	MAPE
L8	1370.25 ± 109.90	967.62 ± 86.067	**56.34**% $\pm$ **7.95**%
S2	1374.01 ± 167.84	1008.11 ± 162.92	$58.11\% \pm 12.19\%$
S1	1478.81 ± 148.82	1019.66 ± 136.36	$61.30\% \pm 10.13\%$
Fusion	1327.31 ± 213.83	961.15 ± 139.91	**57.61**% $\pm$ **14.10**%

Table 24. **Crop yield prediction with actual growing season using U-TAE architecture.** The time-series data prepared using the proposed method is used as an input for estimating the yield of the paddy crops when using the *actual standard growing season*.